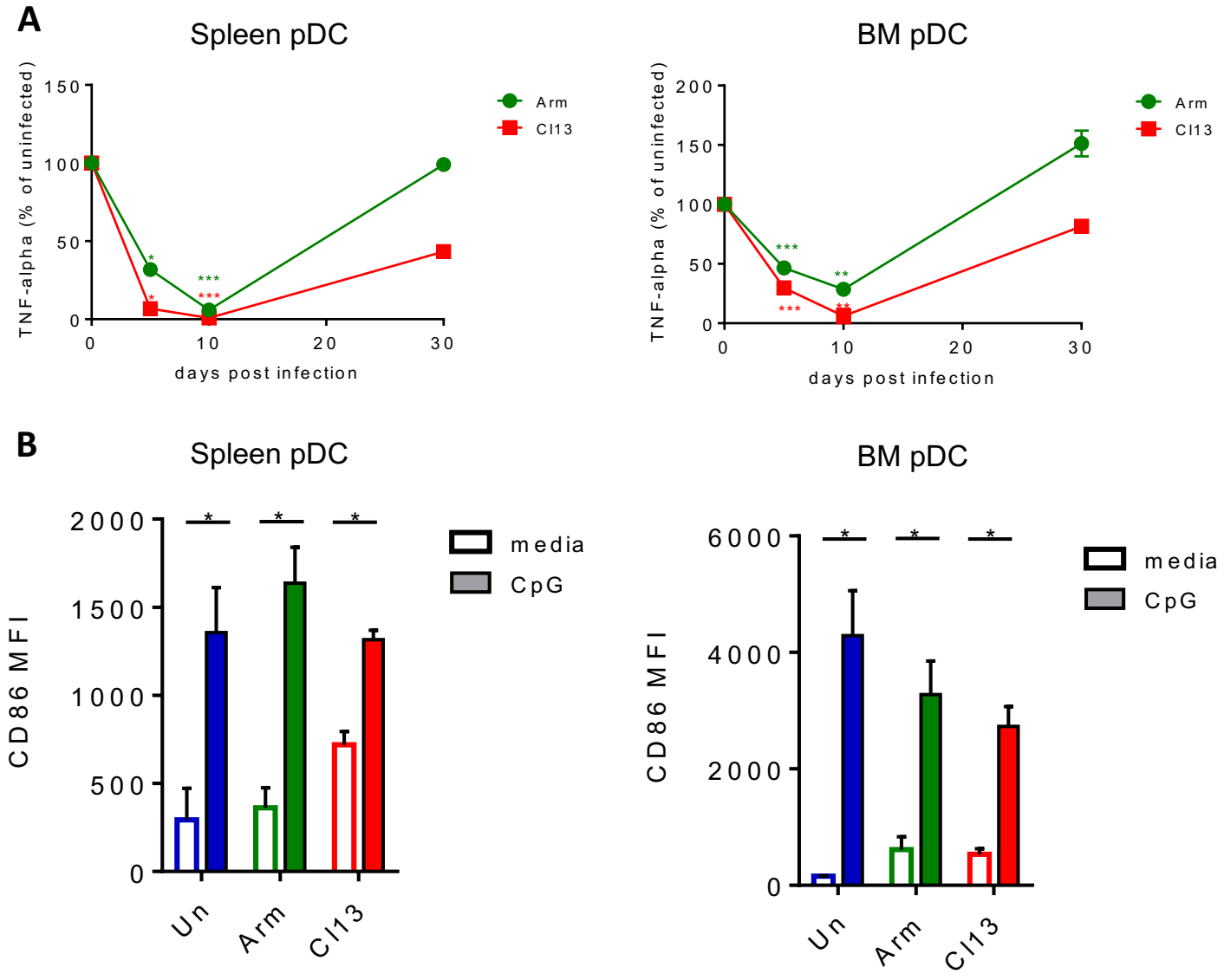

Figure S1. pDCs respond to TLR stimulation, but produce reduced amount of TNF-alpha early during acute and chronic LCMV infection. Related to Figure 1. Wild-type (WT) mice were infected with LCMV ARM (green) or Cl13 (red) or left uninfected (blue) and sacrificed at day 5, 10, and 30 p.i. FACS-purified splenic pDCs (left) or BM pDCs (right) were stimulated with CpG-B 1668 for 15 hours. (A) ELISA was used to quantify TNF-α in the supernatant. Graphs depict the percentage change in TNF-α normalized to uninfected mice processed in parallel at each time point. (B) Flow cytometry was used to evaluate CD86 expression on pDCs. Graphs depict CD86 MFI in spleen pDCs at day 10 p.i. (left) and BM pDCs at day 5 p.i. (right) that were untreated (open bar) or stimulated with CpG-B (filled bar). Graphs depict mean ± SEM. Data are representative of 2-3 independent experiments with 3-10 mice/group. *p<0.05, **p<0.01, ***p<0.001 (one-way Anova to compare ARM-infected (green asterisks) and Cl13-infected group (red asterisks) to uninfected group processed in parallel at each time point (A) or unpaired, two-tailed t-test to compare CpG-B stimulated samples to unstimulated controls (B)).

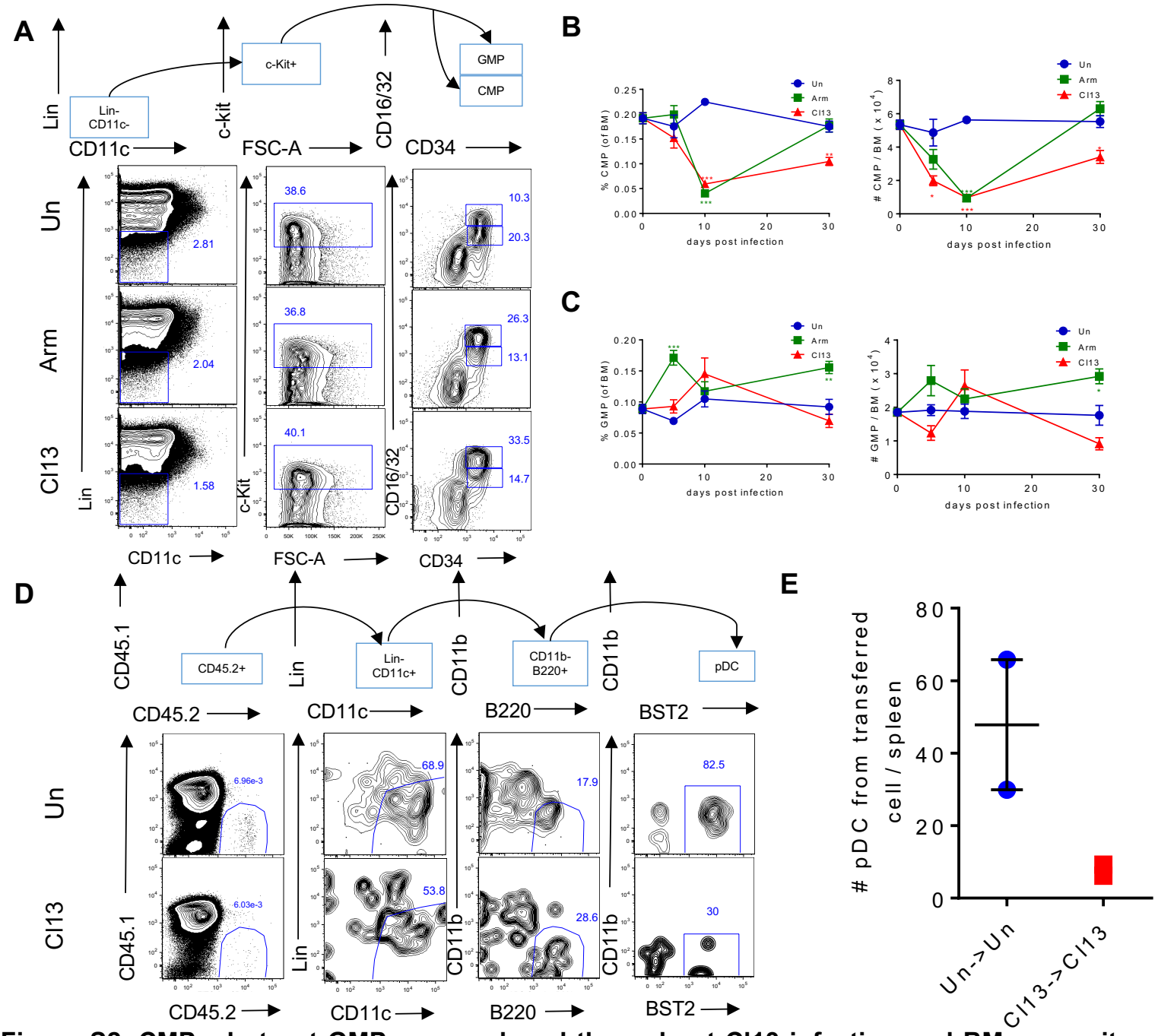

Figure S2. CMPs, but not GMPs, are reduced throughout Cl13 infection and BM progenitors show impaired capacity to generate pDCs *in vivo*. Related to Figure 1. WT mice were infected with LCMV ARM (green) or Cl13 (red) or left uninfected (blue) and sacrificed at days 5, 10, and 30 p.i. (A) Gating strategy and representative FACS plots for CMPs and GMPs in BM at day 10 p.i. where CMPs were identified as Lin$^-$c-kit$^+$CD34$^+$CD16/32^{int} and GMPs as Lin$^-$c-kit$^+$CD34$^+$CD16/32^{hi}. Lin includes markers for Thy1.2, CD19, NK1.1, CD3, CD4, CD8, B220, CD11b, Gr-1, and Ter119. (B-C) Proportions (left) and absolute numbers (right) of CMPs (B) and GMPs (C) in BM. (D-E) FACS-purified Lin$^-$c-Kit$^{int/lo}$Flt3$^+$ progenitors (1.5 x 10^4 cells) from CD45.2$^+$ uninfected or Cl13-infected donor mice at day 30 p.i. were injected intravenously into CD45.1$^+$ non-irradiated uninfected or infection-matched recipients, respectively. Mice were sacrificed at day 10 after transplantation (day 40 p.i.), and spleen cells were analyzed by flow cytometry after T and B cell depletion. (D) Gating strategy and representative FACS plots for donor-derived spleen pDCs within live cells. (E) Absolute numbers of CD45.2$^+$ donor-derived spleen pDCs at day 10 after transplantation. Data are representative of 2-3 independent experiments with 3-5 mice/group (A-C) or pooled from 2 independent experiments where 3-4 mice / group were pooled for analysis in each experiment. *p<0.05, **p<0.01, ***p<0.001 (one-way Anova to compare ARM-infected (green asterisks) and Cl13-infected (red asterisks) groups to uninfected group processed in parallel at each time point (B-C)).

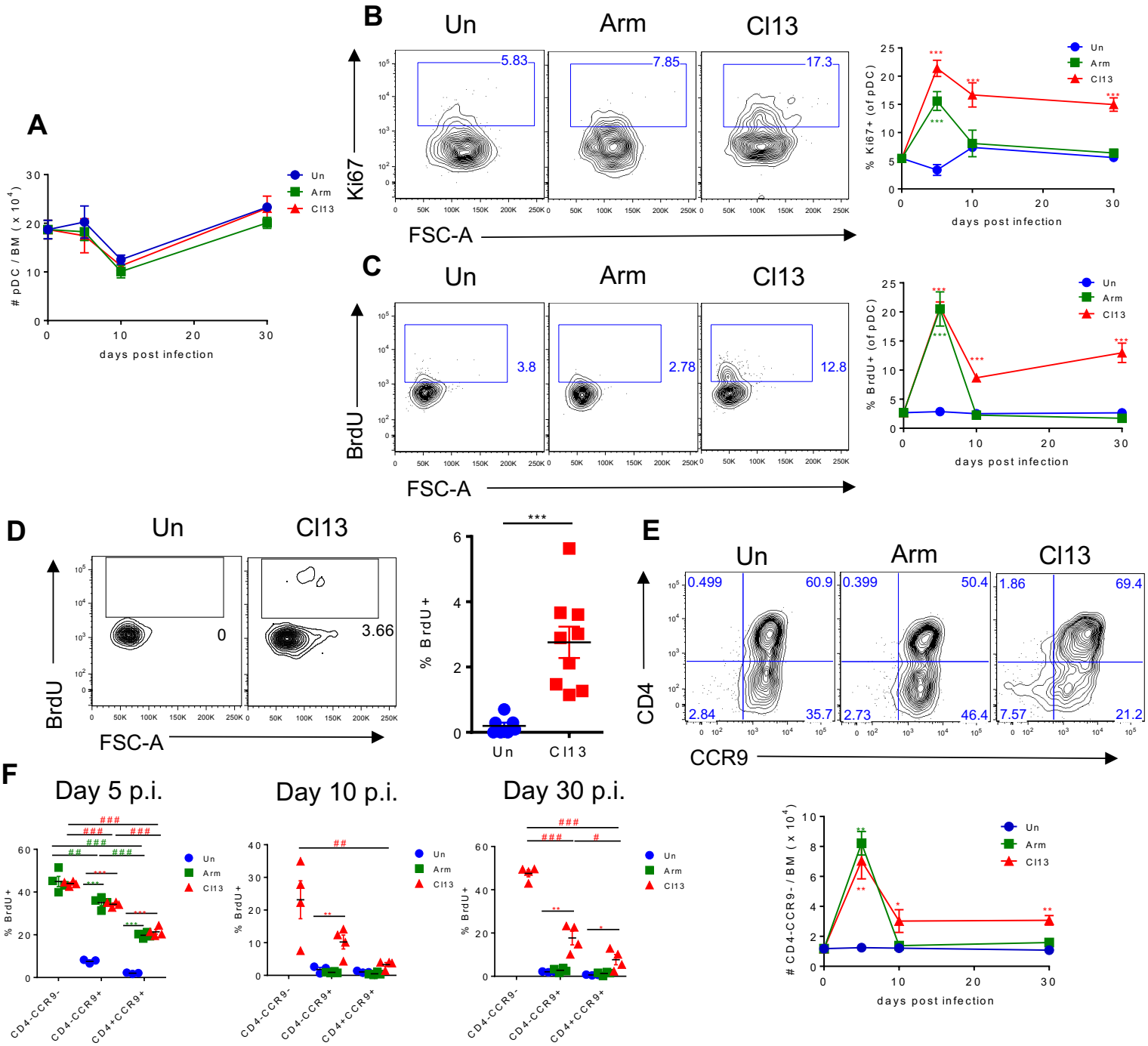

Figure S3. Local proliferation of pDCs with expansion of CD4- pDC subsets is sustained in BM of Cl13 infected mice and splenic pDCs incorporate BrdU *ex vivo*. Related to Figure 2. (A-C, E-F) WT mice were infected with LCMV ARM (green) or Cl13 (red) or left uninfected (blue) and sacrificed at day 5, 10, and 30 p.i. BM pDCs were analyzed to determine their absolute number (A), Ki67 expression (B), BrdU incorporation *in vivo* (C), absolute number of $CD4^{-}CCR9^{-}$ subsets (E) and BrdU incorporation by $CD4^{+}CCR9^{+}$, $CD4^{-}CCR9^{+}$, and $CD4^{-}CCR9^{-}$ subsets at each time point. (F). Representative FACS plots for BM pDCs from day 10 p.i. are shown (B, C, and E). (D) WT mice were infected with LCMV Cl13 (red) or left uninfected (blue) and sacrificed at day 9 p.i. Representative FACS plots for BrdU incorporation by splenic pDCs after 7 hour *ex vivo* culture in the presence of BrdU. Graphs depict mean ± S.E.M . and symbols represent individual mice. Data are representative of 2-3 independent experiments with 3-5 mice/group (A-C, E-F). Data are pooled from 2 independent experiments with 3-5 mice/group (D). *, # $p<0.05$, **, ## $p<0.01$, ***, ### $p<0.001$ (one-way Anova to compare ARM-infected (green asterisks) and Cl13-infected (red asterisks) group to uninfected group processed in parallel at each time point (A-C, E-F) or to compare $CD4^{+}CCR9^{+}$, $CD4^{-}CCR9^{+}$, and $CD4^{-}CCR9^{-}$ subpopulations in ARM-infected (green pounds) or Cl13-infected group (red pounds) (F) or unpaired, two-tailed t-test (D)).

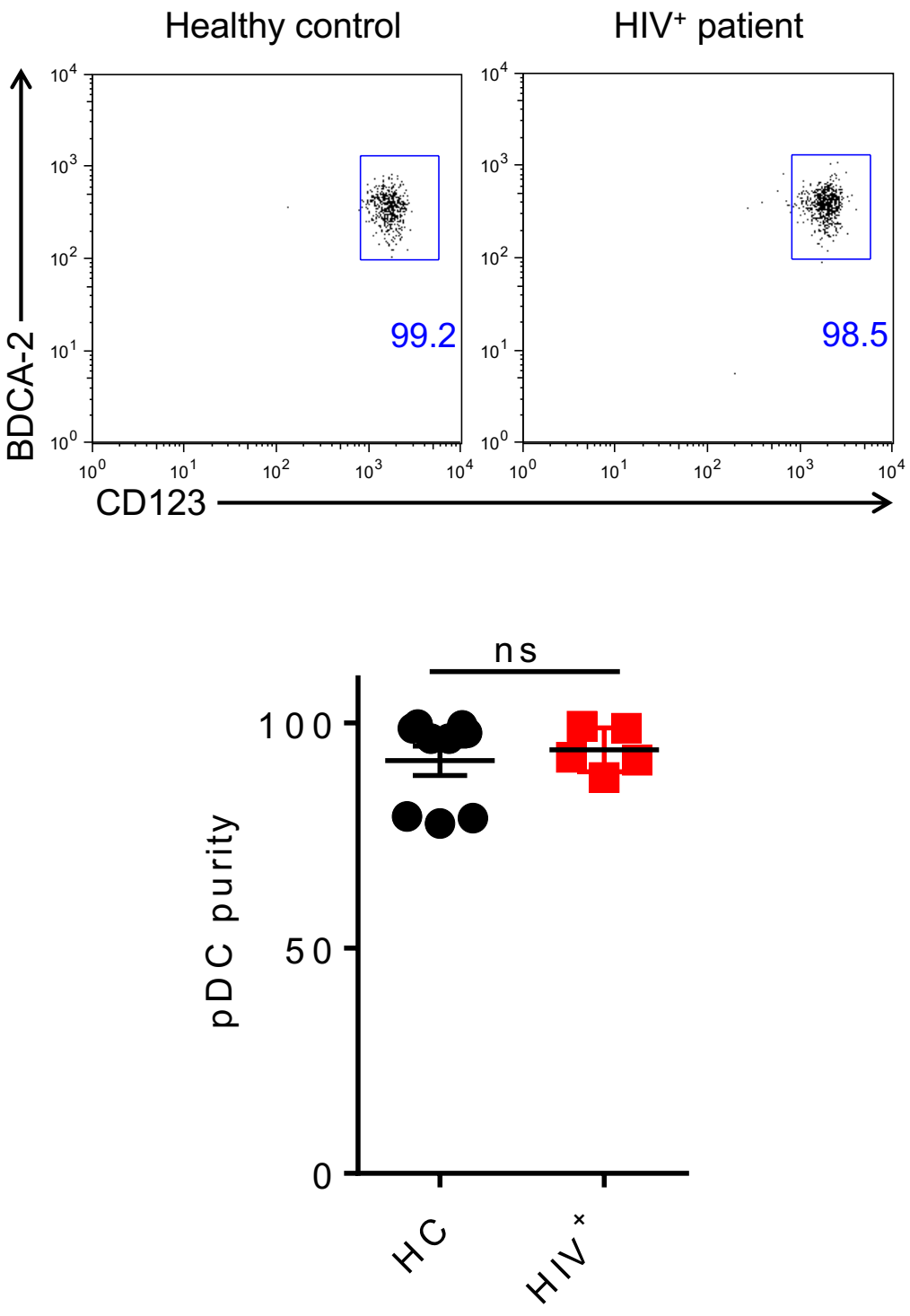

Figure S4. Purity of pDCs isolated from healthy controls and HIV infected patients are not different. Related to Figure 3. (A) Representative FACS plots of pDCs isolated from healthy controls (left panel) and HIV+ patients (right panel). (B) Purity of pDCs isolated from healthy controls (HC; black) and HIV+ patients (HIV+; red). Graph depicts mean ± SEM and symbols represent individual donors. ns, not significant (unpaired, two-tailed t-test).

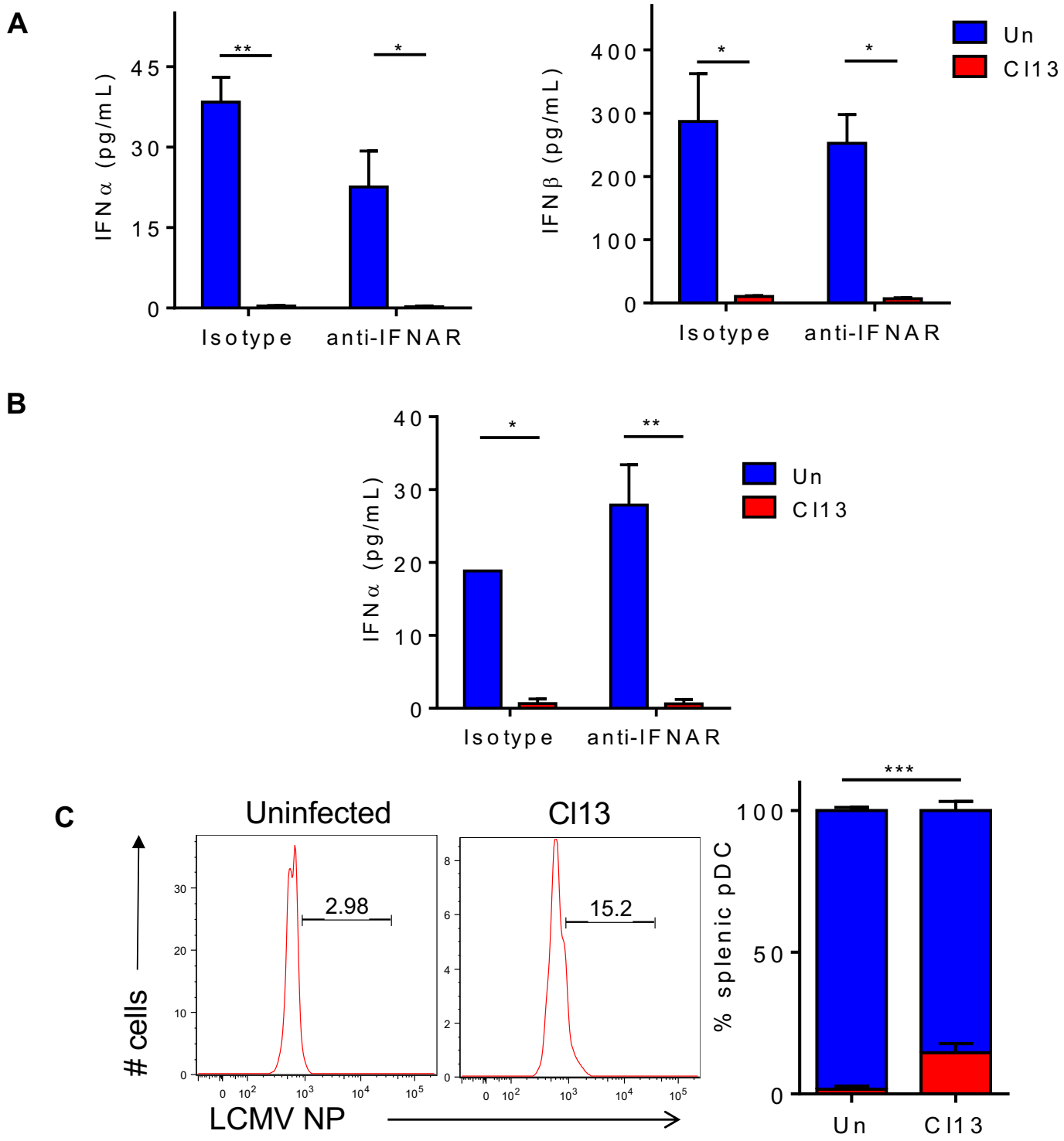

Figure S5. Functional exhaustion of pDCs is not caused by IFN-I signaling or overwhelming NP expression in pDCs. Related to Figure 6. (A-B) WT mice were treated with isotype or anti-IFNAR nAb beginning 1 day before and throughout LCMV Cl13 infection and sacrificed at day 9 p.i. (A) BM was cultured with Flt3L (continuing treatment with isotype or anti-IFNAR nAb *in vitro*) and at day 8 post-culture, FACS-purified pDCs were stimulated with CpG-B for 15 hours. Levels of IFNα (left) and IFNβ (right) were determined in culture supernatants by ELISA. (B) FACS-purified splenic pDCs were stimulated with CpG-B for 6 hours and supernatants were evaluated for IFNα by ELISA. (C) WT mice were infected with LCMV Cl13 or left uninfected. LCMV NP expression was quantified by flow cytometry at day 9 p.i. Representative histograms are shown and graphs depict percentage of splenic pDCs that are NP negative (blue) or positive (red). Data are representative of 2 independent experiments where 4-7 mice/group were pooled (A-B) or with 3 mice/group (C). Bars depict mean ± SEM. *p<0.05, **p<0.01, ***p<0.001 (two-way Anova (A-B) or unpaired, two-tailed t-test (C)).

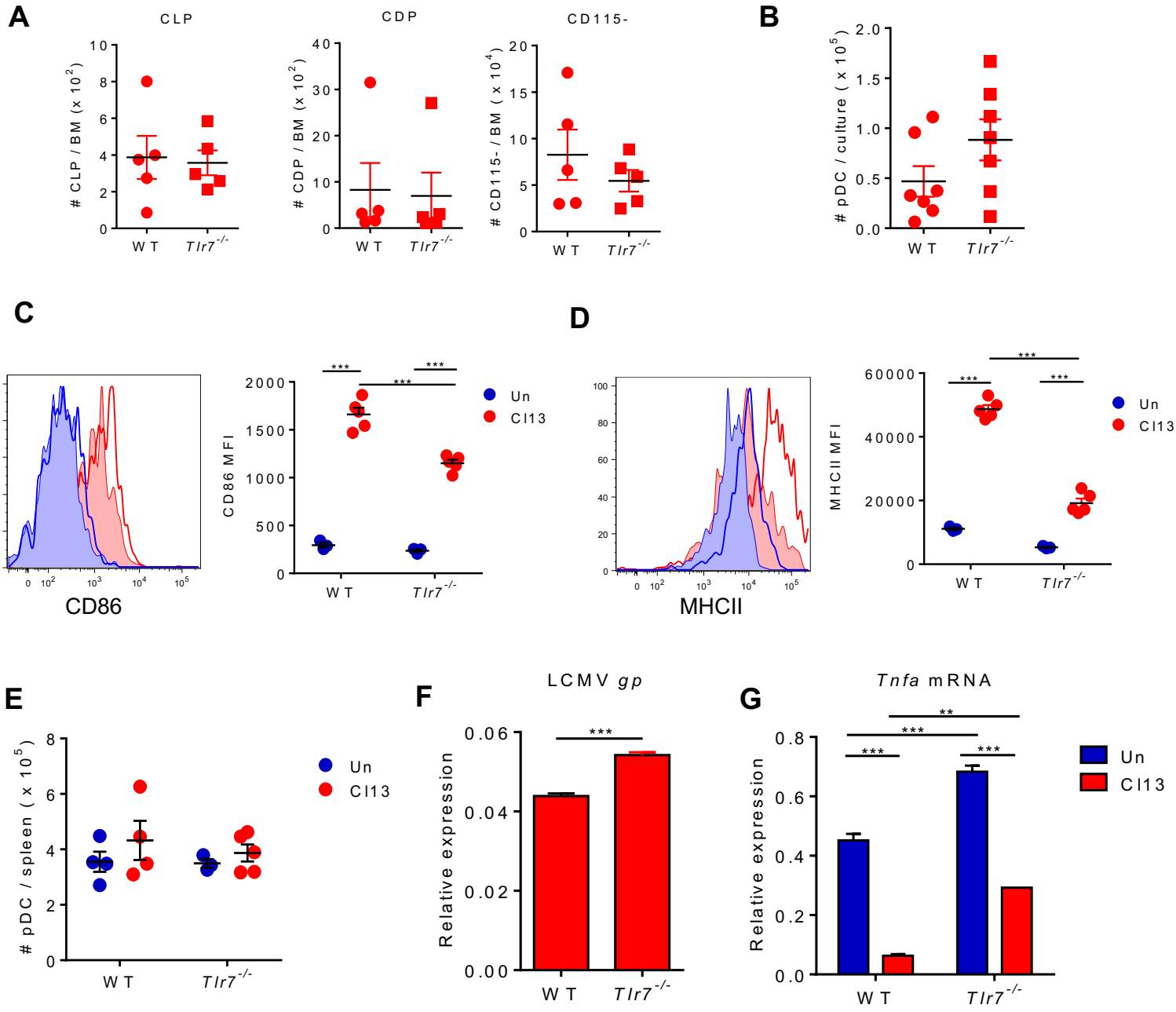

Figure S6. TLR7 signaling does not affect number and developmental potential of BM pDC progenitors, but induces maturation and decreases TNFa production in pDCs despite positively regulating viral control. Related to Figure 6. (A-F) WT and *Tlr7*$^{-/-}$ mice were left uninfected (blue) or infected with LCMV Cl13 for 9 days (red). Absolute number of indicated BM progenitors (A) or pDCs generated from BM-Flt3L-cultures (B) were determined. Representative histograms of CD86 (C) and MHCII (D) expression on splenic pDCs from WT uninfected mice (blue open), *Tlr7*$^{-/-}$ uninfected mice (blue filled), WT Cl13-infected (red open) and *Tlr7*$^{-/-}$ Cl13-infected (red filled) mice are shown. Graphs depict MFI of CD86 (C) and MHCII (D). Absolute number of splenic pDCs was determined (E). pDCs from infected mice were evaluated for LCMV *gp* transcript relative to *Gapdh* (F). (G) Mixed BM chimeras were generated using BM from WT (CD45.1^{+}) and *Tlr7*$^{-/-}$ (CD45.2^{+}) mice and infected with LCMV Cl13 for 9 days. FACS-purified splenic pDCs were stimulated with CpG-B and evaluated for *Tnfa* transcripts relative to *Gapdh*. Data are representative of 2 independent experiments with 3-5 mice/group (A, C-G) or pooled from 5 experiments where 4-7 mice were pooled into 1-2 groups in each experiment (B). Bars depict mean ± SEM. Symbols represent individual mice. **p<0.01, ***p<0.001 (unpaired, two-tailed t-test (A-B, F) or two-way Anova (C-E, and G)).

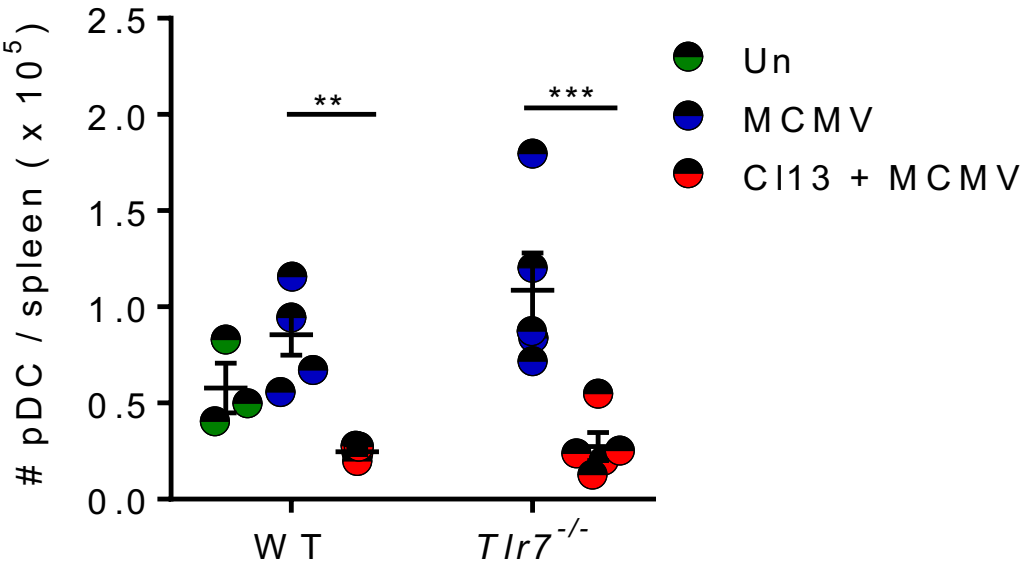

Figure S7. pDC numbers are reduced upon secondary infection of Cl13 infected mice but this reduction is not mediated by TLR signaling. Related to Figure 7. Uninfected and LCMV Cl13-infected WT and TLR7ko mice (day 20 p.i.) were infected with MCMV and sacrificed at day 3.5 post MCMV infection. Graph depicts mean ± SEM of absolute numbers of splenic pDCs and symbols represent individual mice. Data are representative of 2 independent experiments with 3-4 mice/group. **p<0.01, ***p<0.001 (two-way Anova).

Donor Type	Sex	Age	On cART	HIV-1 RNA (copies /ml)	CD4 count / mm^3
Healthy Control	M	30			
	M	50			
	F	50			
	M	50			
	M	50			
	F	50			
	M	50			
	M	50			
	F	50			
HIV+ patient	M	50	YES	56335	40
	F	55	YES	39088	328
	M	49	YES	5917	396
	M	53	NO	900	263
	F	48	YES	32592	160

Table S1. Related to Figure 3. Clinical summary of human samples used in this study

qPCR Primers		
Name	**Primer-Forward**	**Primer-Reverse**
Gapdh **(Taqman with probe #9)**	AGCTTGTCATCAACGGGAAG	TTTGATGTTAGTGGGGTCTCG
Tcf4 **(Taqman with probe #9)**	ATTTGTGGCCATTGAAGGTT	GTCCCTAAGGCAGCCATTC
Gapdh	CATGGCCTTCCGTGTTCCTA	CCTGCTTCACCACCTTCTTGAT
Spib	AAATCCGCAAGGTCAAACGC	TTCAGGGGGAGTACAGAGGG
Bcl11a	TGGTATCCCTTCAGGACTAGGT	TCCAAGTGATGTCTCGGTGGT
Ifnα	TATGTCCTCACAGCCAGCAG	TTCTGCAATGACCTCCATCA
Ifnβ **(Taqman with probe #18)**	CTGGCTTCCATCATGAACAA	AGAGGGGGTGGTGGAGAA
Tnfα	CCCTCACACTCAGATCATCTTCT	GCTACGACGTGGGCTACAG
LCMVsSgp1	CATTCACCTGGACTTTGTCAGACTC	GCAACTGCTGTGTTCCCGAAA
TCF4	CAGCTATGCCTGGTGGTCAT	GTCCCCACCATGAGTGAATGT
SPIB	GGAGTGCTGCCCTGCCATAA	CCCCCACCCCAGATGAGATT
BCL11A	TATGCCCCGCAGGGTATTTG	CTTCCGTGTTCGCTTTCTAAGTA
GAPDH	TGATGACATCAAGAAGGTGGTGAAG	TCCTTGGAGGCCATGTGGGCCAT

Table S2. Related to STAR method. Sequences of the qPCR primers used in this study.